THE JOURNAL OF BIOLOGICAL CHEMISTRY
© 1992 by The American Society for Biochemistry and Molecular Biology, Inc.

Vol. 267, No. 31, Issue of November 5, pp. 22662-22672, 1992
Printed in U.S.A.

Expression and Function of IRS-1 in Insulin Signal Transmission*

(Received for publication, May 12, 1992)

Xiao Jian Sun‡, Montserrat Miralpeix§, Martin G. Myers, Jr.¶, Erin M. Glasheen, Jonathan M. Backer‖, C. Ronald Kahn, and Morris F. White

From the Research Division, Joslin Diabetes Center and the Department of Medicine and Program in Cellular and Developmental Biology, Harvard Medical School, Boston, Massachusetts 02215

IRS-1 is a major insulin receptor substrate which may play an important role in insulin signal transmission. The mRNA for IRS-1 in rat cells and tissues is about 9.5 kilobases (kb). Rat liver IRS-1 was stably expressed in Chinese hamster ovary (CHO) cells (CHO/IRS-1). Although its calculated molecular mass is 131 kDa, IRS-1 from quiescent cells migrated between 165 and 170 kDa during sodium dodecyl sulfate-polyacrylamide gel electrophoresis. IRS-1 was phosphorylated strongly on serine residues and weakly on threonine residues before insulin stimulation. Insulin immediately stimulated tyrosine phosphorylation of IRS-1, and after 10–30 min with insulin its apparent molecular mass increased to 175–180 kDa. Expression of the human insulin receptor and rat IRS-1 together in CHO/IR/IRS-1 cells increased the basal serine phosphorylation of IRS-1 and strongly increased tyrosine phosphorylation during insulin stimulation. Purified insulin receptors directly phosphorylated baculovirus-produced IRS-1 exclusively on tyrosine residues. By immunofluorescence, IRS-1 was absent from the nucleus, but otherwise distributed uniformly before and after insulin stimulation. Some IRS-1 associated with the insulin receptor during insulin stimulation. In addition, a phosphatidylinositol 3′-kinase associated with IRS-1 during insulin stimulation, and this association was more sensitive to insulin in CHO cells overexpressing the insulin receptor (CHO/IR cells), more responsive to insulin in CHO/IRS-1 cells, and both sensitive and responsive in CHO/IR/IRS-1 cells. Similarly, insulin-stimulated DNA synthesis was more sensitive to insulin in CHO/IR cells, and more responsive in CHO/IRS-1 cells; however, insulin-stimulated DNA synthesis was sensitive but poorly responsive to insulin in CHO/IR/IRS-1 cells. Together, these results suggest that IRS-1 is a direct physiologic substrate of the insulin receptor and may play an important role in insulin signal transmission.

Insulin signal transmission is initiated by hormone binding to the α-subunit of the insulin receptor, which activates the tyrosine kinase in the β-subunit (1, 2). Although many details of the structure and function of the insulin receptor are understood, the molecular events that link the receptor to cellular enzymes and the glucose transport system have been difficult to identify. Based on the hypothesis that the early components in the pathway of insulin action undergo tyrosine phosphorylation, we utilized anti-phosphotyrosine antibodies (αPY)[1] to identify these proteins in insulin-stimulated cells (3). Insulin immediately stimulates tyrosine phosphorylation of a protein between 165 to 185 kDa, called pp185 (3). Tyrosine phosphorylation of pp185 requires kinase-active receptors (4); it is strongly phosphorylated in cells expressing high levels of insulin receptors, but decreased in cells expressing mutant receptors defective in signaling (5, 6). Other cellular proteins have been identified as insulin receptor substrates, including pp120 in rat liver (7), pp15 in 3T3-L1 cells and adipocytes (8–10), and pp46 in adipocytes (11). However, pp185 is found in these and many other cells and tissues suggesting that it may play a general role in insulin signal transmission (5, 12–17).

Recently, we purified pp185 from insulin-stimulated rat liver by affinity chromatography on immobilized anti-phosphotyrosine antibody (18), and using partial amino acid sequence data we isolated a cDNA molecule encoding this protein (19). The cloned protein, called IRS-1, shows no significant amino acid sequence identity to known proteins. There is a 90.5% amino acid sequence identity between rat and human IRS-1, and all the identified structural motifs are conserved (19, 20). IRS-1 is hydrophilic with no stretch of hydrophobic residues long enough to provide a transmembrane spanning region, consistent with the cytosolic location of pp185 (5). IRS-1 has a calculated molecular mass of 131 kDa and over 30 potential serine and threonine phosphorylation sites. Moreover, it contains 14 potential tyrosine phosphorylation sites, six of which are found in YMXM (Tyr-Met-Xaa-Met) motifs, and three in YXXM motifs (19, 21). Phosphorylated YMXM motifs are thought to associate with certain proteins containing SH2 (src homology-2) domains (19, 22).

IRS-1 undergoes tyrosine phosphorylation immediately after insulin stimulation and associates with the phosphati-

* This work was supported in part by National Institutes of Health Grants DK33201 (to C. R. K.) and DK43808 (to M. F. W.) and by Endocrinology Research Center Grant DK 36836 to the Joslin Diabetes Center. The costs of publication of this article were defrayed in part by the payment of page charges. This article must therefore be hereby marked "*advertisement*" in accordance with 18 U.S.C. Section 1734 solely to indicate this fact.

‡ Supported by the Juvenile Diabetes Foundation.

§ Recipient of a postdoctoral fellowship from the Ministry of Education and Science (Spain).

¶ Partially supported by the Medical Scientist Training Program at Harvard Medical School.

‖ Recipient of a Career Development Award from the American Diabetes Association.

[1] The abbreviations used are: αPY, anti-phosphotyrosine antibodies; CHO, Chinese hamster ovary; CHO^n, neomycin-resistant CHO; CHO^n/IR, neomycin-resistant CHO cells expressing 10^6 human insulin receptors; PtdIns 3-kinase, phosphatidylinositol 3-kinase; PtdIns(3)P, phosphatidylinositol (3)-phosphate; PtdIns(3,4)P_2, phosphatidylinositol (3,4,5)-diphosphate; PtdIns(3,4,5)P_3, phosphatidylinositol (3,4,5)-triphosphate; SDS-PAGE, sodium dodecyl sulfate-polymerase chain reaction; PCR, polymerase chain reaction; DTT, dithiothreitol; BSA, bovine serum albumin; TPCK, L-1-tosylamido-2-phenylethyl chloromethyl ketone; TRITC, tetramethylrhodamine isothiocyanate; CHO^{nh}, neomycin- and histidinol-resistant CHO.

dylinositol 3′-kinase (PtdIns 3′-kinase) (19). The PtdIns 3′-kinase phosphorylates the D-3 position of phosphatidylinositol forming PtdIns(3)P, PtdIns(3,4)P_2, and PtdIns(3,4,5)P_3 in the intact cell, which may be involved in the control of cellular growth and metabolism (22–24). The PtdIns 3′-kinase contains two SH2 domains in its 85-kDa subunit (p85), which bind to phosphotyrosine residues in IRS-1.[2] Moreover, association with tyrosyl-phosphorylated IRS-1 activates the PtdIns 3′-kinase *in vitro* and *in vivo* (41). Together these results suggest that IRS-1 is a unique substrate of the insulin receptor kinase which may act as a "docking" protein following its tyrosine phosphorylation. The association of IRS-1 with cellular enzymes that contain the correct SH2 domain isoform may play an important role in the molecular link between the insulin receptor and enzymes controlling cellular growth and metabolism.

In this report, we explore the function of rat liver IRS-1 expressed in Chinese hamster ovary (CHO) cells. In quiescent cells, IRS-1 migrated at 165 kDa during SDS-PAGE and was phosphorylated on multiple serine and threonine residues. During insulin stimulation, IRS-1 was tyrosine phosphorylated in intact cells and migrated near 180 kDa. It is a direct substrate for the insulin receptor as IRS-1 is tyrosine phosphorylated by the insulin receptor in a mixture of partially purified components. Immunofluorescence indicated that IRS-1 was distributed throughout the cytoplasm before and after insulin stimulation; however, a portion of it associated with the activated insulin receptor during immunoprecipitation. Elevated expression of IRS-1 increased the response of CHO cells to insulin stimulation, as both the amount of PtdIns 3′-kinase in anti-IRS-1 immunoprecipitates and insulin-stimulated thymidine incorporation increased. These result are consistent with a role for IRS-1 in insulin signal transmission.

EXPERIMENTAL PROCEDURES

Characterization of IRS-1 Transcripts—Total RNA was isolated from rat tissues by guanidinium isothiocyanate-cesium chloride centrifugation (25). For Northern blot analysis, poly(A)$^+$ RNA was collected on a oligo(dT)-cellulose type 3 column (Collaborative Research) and denatured with 6% formaldehyde (Sigma), size-fractionated by 1% agarose gel electrophoresis, and transferred to nitrocellulose (25). The cDNA probes were prepared by the Multiprime DNA labelling system (Amersham). The cDNA (25 ng) was denatured by heating to 95–100 °C for 2 min and mixed with 5 μl of random hexanucleotides, 5 μl of [^{32}P]dCTP (3000Ci/mmol) (Du Pont-New England Nuclear), and 2 μl of Klenow polymerase in 50 μl of labeling buffer and incubated at 37 °C for 30 min. The labeled cDNA (40–80 × 10^6 cpm) was separated from primer and free [^{32}P]dCTP on a NICK column (Pharmacia LKB Biotechnology Inc.). Hybridizations were performed overnight at 42 °C with 10^6 cpm/ml cDNA in 4 × SSC (0.6 M NaCl, 0.06 M sodium citrate, pH 7.0) containing 0.8 × Denhard's solution, 40% formamide, 7 mM Tris-HCl (pH 7.0), 10% dextran sulfate, and 20 μg/ml salmon sperm DNA. The blots were washed three times at 22 °C in 1 × SSC containing 0.1% SDS and then for 30 min with 0.1 × SSC containing 0.1% SDS at 51 °C. The nitrocellulose membranes were exposed to Kodak XAR-5 film for 6 days at −80 °C with a Quanta 111 intensifying screen.

IRS-1 c-DNA Constructions—A cDNA containing the full-length open reading frame of IRS-1 was assembled in pBluescript (Stratagene) from four partial cDNA inserts (called P-9, C-18, P-2-2, and S-15 in Ref. 26) by using *Bst*EII, *Afl*III, and *Aat*II restriction sites. The correct orientation of each fragment in the full-length IRS-1 cDNA was verified by restriction mapping, and the complete IRS-1 cDNA was confirmed by DNA sequencing (United States Biochemicals). The 5′-noncoding region of the IRS-1 cDNA was removed, because it contains several possible in-frame start and stop codons which might interfere with the efficient translation. In order to remove these regions, the sequence from 553 to 997 including the start codon at 588 and *Bst*EII site at 642 was amplified by the polymerase chain reaction (27). The 5′-end primer located at 553 was adapted with an *Spe*I site (tcaact AGT TTT TCG ACA CCT CCC TCT GCT C); the 3′-end primer was located at nucleotide 997 (CAG AGC TGC CGC TGC A) in the IRS-1 cDNA (Oligos Etc. Inc.). PCR was performed in 100 μl of 100 mM Tris-HCl (pH 8.3) containing 50 mM KCl, 1.5 mM $MgCl_2$, 0.01% gelatin, 0.2 mM dNTP, 50 pmol of primers, 0.5 μg of full-length IRS-1 cDNA in pBluescript, and 2.5 units of Taq DNA polymerase (Perkin-Elmer/Cetus). The reaction was cycled 10 times at 94 (1 min), 55 (2 min), and 72 °C (1.5 min), and the PCR products were cut with *Spe*I and *Bst*EII. The 5′-end of IRS-1 was removed from pBluescript by digestion with *Spe*I (in the pBluescript polylinker region) and *Bst*EII (nucleotide 642) and replaced with the fragment (553–642) released from the PCR product. The new vector which carried the modified IRS-1 cDNA was confirmed by sequencing and restriction mapping.

In Vitro Translation of the IRS-1 cDNA—IRS-1 mRNA was synthesized using full-length or 5′-end truncated IRS-1 cDNA in linearized pBluescript. The cDNA was linearized at the 3′-end by digestion with *Eco*RV to include the cloned 3′-untranslated region in the mRNA, or linearized with *Aat*II in order to truncate the 3′-untranslated region immediately after the first stop codon (See the diagram in Fig. 2*A*). *In vitro* transcription was performed at 37 °C for 60 min in 100 μl of transcription buffer (20 mM Tris-HCl, pH 7.5, 3 mM $MgCl_2$, 1 mM spermidine, and 5 mM NaCl) containing 10 mM DTT, 0.1 mg/ml RNase-free BSA (Promega), 0.5 mM ATP, CTP, UTP, and 0.05 mM GTP, 0.5 mM GpppG (Promega), 120 units of RNasin ribonuclease inhibitor (Promega), 5 μg of linearized IRS-1 cDNA and 40 units of T3 RNA polymerase (Promega). The cDNA was removed by adding 5 units of RNase-free DNase (Promega) and incubated at 37 °C for 15 min. The newly synthesized mRNA was analyzed on formaldehyde agarose gels and showed the expected sizes.

In vitro translation of IRS-1 mRNA was performed at 30 °C for 2 h in 50 μl of reaction mixture containing 35 μl of nuclease-treated rabbit reticulocyte lysate (Promega), 40 units of RNasin ribonuclease inhibitor, 1 μl of 1 mM methionine-free amino acid mixture (Promega), 3 μg of synthesized mRNA that was denatured at 67 °C for 10 min, and 4 μl of *trans*-label [^{35}S]methionine (10 mCi/ml; Du Pont-New England Nuclear). The translation products were analyzed directly by 6% SDS-PAGE or immunoprecipitated first before SDS-PAGE and detected by autoradiography.

Expression of IRS-1 c-DNA in CHO Cells—The 5′-truncated IRS-1 cDNA prepared above was released from pBluescript by digestion with *Spe*I and *Eco*RV and inserted into pCMVhis (19) at a blunt-ended *Hin*dIII site to form pCMVhis/IRS-1. The pCMVhis expression vector confers histidinol resistance to CHO cells (28). Neomycin-resistant Chinese hamster ovary (CHO^n) cells and neomycin-resistant CHO cells expressing 10^6 human insulin receptors (CHO^n/IR) were transfected with pCMVhis or pCMVhis/IRS-1 (10 μg) and selected by resistance to 10 mM histidinol (Sigma). Two G418- and histidinol-resistant CHO^{nh} cell lines expressing IRS-1 alone (CHO^{nh}/IRS-1) and four cell lines expressing both the insulin receptor and IRS-1 (CHO^{nh}/IR/IRS-1) were selected which expressed nearly equivalent amounts of IRS-1 (within 30%) as demonstrated by [^{35}S]methionine labeling and αIRS-1 immunoblotting. A single clone of histidinol-resistant CHO^{nh} and CHO^{nh}/IR cells were shown to behave identically to CHO^n and CHO^n/IR, respectively. Although we have omitted the "nh" superscript indicating G418 and histidinol resistance for simplicity, all cell lines used in the study contain this double-drug resistance.

[^{35}S]Methionine and [^{32}P]Phospate Labeling—Confluent monolayers of transfected cells in 15-cm dishes (Nunclon) were labeled for 15 h at 37 °C with 15 ml of 0.1 mCi/ml Trans^{35}S-label (Du Pont-New England Nuclear) or for 3 h at 37 °C with 10 ml of 0.4 mCi/ml [^{32}P] orthophosphate (Du Pont-New England Nuclear). The cells were incubated for an additional 2 min in the absence or presence of 100 nM insulin and rapidly frozen with liquid nitrogen. The frozen cells were solubilized in 100 mM Tris-HCl (pH 7.5) containing 2 mM sodium orthovanadate, 0.34 mg/ml phenylmethylsulfonyl fluoride, 100 μg/ml aprotinin, 10 mM sodium pyrophosphate, 100 mM sodium fluoride, 5 mM EDTA, and 1% Triton X-100. IRS-1 was immunoprecipitated as previously described with anti-peptide antibody raised against Y^{489}IPGATMGTSPALTGDEA of rat IRS-1 (αIRS-1) or antiphosphotyrosine antibody (αPY) (19). The immunoprecipitates were washed with 50 mM HEPES (pH 7.4) containing 1% Triton X-100, 0.1% SDS, 150 mM NaCl, 100 mM NaF, and 2 mM sodium

[2] Myers, M. G., Jr., Backer, J. M., Sun, X. J., Shoelson, S., Hu, P., Schlessinger, J., Yoakim, M., Schaffhausen, B., and White, M. F. (1992) *Proc. Natl. Acad. Sci. U.S.A.*, in press.

orthovanadate; in some cases the SDS was omitted to maintain the association between IRS-1 and the insulin receptor. Immunoprecipitated proteins were reduced with dithiothreitol, separated on one-dimensional 7.5% SDS-PAGE at 100 V (constant), and detected by autoradiography.

Tryptic Peptide Mapping of [^{32}P]IRS-1—Polyacrylamide-gel fragments containing the [^{32}P]IRS-1 were washed for 15 h at 37 °C with 20 ml of 20% (v/v) methanol to remove SDS. The gel was dried at 70 °C for 60 min and rehydrated in 1 ml of 50 mM NH_4HCO_3 containing 100 μg of TPCK-treated trypsin (Worthington Biochemical Corp). The mixture was incubated for 20 h at 37 °C followed by an additional 4-h incubation with 50 μg of trypsin. The gel fragments were removed, and the supernatant was clarified by centrifugation (10,000 × *g* for 5 min). The supernatant was freeze-dried, and the residue was dissolved in 100 μl of 0.055% trifluoroacetic acid and clarified by centrifugation. The phosphopeptides were separated in a Beckman Gold System equipped with an Hi-Pore reversed-phase RP-318 column (Bio-Rad) eluted at a flow of 1 ml/min with 0.055% trifluoroacetic acid (Solution A) modified with 75% acetonitrile-0.05% trifluoroacetic acid (Solution B). The radioactivity (Cerenkov) eluted from the column in 0.5-ml fractions was measured in a Beckman LS 1801 scintillation counter.

Phosphoamino Acid Analysis—The phosphoamino acid composition of [^{32}P]IRS-1 separated from ^{32}P-labeled CHO cells by immunoprecipitation and SDS-PAGE was carried out as previously described (29). Phosphoproteins were eluted from the gel fragments by trypsin digestion and were hydrolyzed in 6 N HCl at 110 °C for 120 min. The amino acid mixture was separated by thin-layer electrophoresis on microcellulose plates developed at 1000 V (constant) in H_2O/acetic acid/pyridine (89:10:1). The phosphoamino acid standards (Sigma) were detected by reaction with ninhydrin, and the radioactive amino acids were detected by autoradiography.

Immunoblotting—Cell lysates or immunoprecipitated proteins were separated by 6% SDS-PAGE at 100 V (constant), and transferred to nitrocellulose (Schleicher & Schuell) at 100 V (constant) for 2 h at 5–15 °C in the Bio-Rad Mini-Protean apparatus. The transfer was carried out in Towbin buffer containing 0.02% SDS. The nitrocellulose was incubated at 4 °C overnight in TNA (10 mM Tris (pH 7.2), 0.9% NaCl, and 0.02% NaN_3) containing 3% bovine serum albumin (blocking buffer), and then with the indicated antibody (2 μg/ml) diluted in blocking buffer for 2 h at 22 °C. The nitrocellulose was washed three times for 15 min each in TNA containing 0.01% Tween-20 and then incubated with 2 μCi of [^{125}I]protein A (ICN) in 10 ml of blocking buffer for 1 h at 22 °C. Bound antibodies were detected by autoradiography using Kodak XAR film with Cronex Lightning Plus intensifying screens at −70 °C for 4–12 h.

Expression of IRS-1 in Sf9 Cells and in Vitro Phosphorylation of IRS-1 by Purified Insulin Receptor—The cDNA for IRS-1 was subcloned into pBluescript using the 5′-*Spe*I and 3′-*Hin*dIII sites on IRS-1 and complementary sites in the polylinker of pBluescript vector. Most of the 3′-untranslated region was removed by digestion with *Aat*II and *Hin*dIII. The vector was then ligated with a linker containing *Aat*II and *Hin*dIII ends and an intervening *Spe*I cut site. All of the 5′-untranslated sequences were removed by digestion with *Sac*I which cuts in the pBluescript vector, and *Bsp*EI which cuts immediately after the translation start site. The vector was ligated with a linker containing *Sac*I and *Bsp*EI ends, an *Nhe*I site just before the translation start site, and coding sequences which had been removed. The coding sequences of the IRS-1 cDNA were then excised by digestion with *Nhe*I and *Spe*I and ligated into the *Nhe*I cloning site of pBlueBac (Invitrogen) producing pBB/IRS-1. Recombinant baculovirus containing IRS-1 cDNA in place of the viral polyhedrin gene was obtained from Sf9 cells transfected with pBB/IRS-1 (30).

Sf9 cells grown in TNM-FH (Sigma) supplemented with 10% fetal bovine serum were infected at high multiplicity with a recombinant baculovirus. After 50–54 h, the cells were harvested by low speed centrifugation, and the cell pellet was lysed in a Dounce homogenizer (20 strokes) in 50 mM Tris-HCl (pH 7.8) containing 1 M NaCl, 1 mM phenylmethylsulfonyl fluoride, 1 mM benzamidine, 10 μg/ml aprotinin, and 10 μg/ml leupeptin. Insoluble material was removed by centrifugation at 100,000 × *g* for 1 h. The supernatant containing IRS-1 protein (IRS-1^{bac}) was purified partially on SK 300 HR gel filtration media (Pharmacia). The peak fraction typically contained approximately 0.5 mg/ml IRS-1 with a purity of ~90% as determined by scanning densitometry of Coomassie Blue-stained polyacrylamide gels.

Insulin receptor from 5–8 μg of wheat germ agglutinin-purified protein from CHO/IR cells was autophosphorylated for 20 min by incubation in 50 mM Tris-HCl (pH 7.8) containing 1 M NaCl, 5 mM $MnCl_2$, 50 μM ATP (20–50 μCi of [γ-^{32}P]ATP) in the presence of 100 nM insulin (31). IRS-1^{bac} (2 μg) was then incubated with or without the insulin receptor for the indicated time intervals. Reactions were stopped by boiling with one volume of 2 × Laemmli sample buffer for 5 min before loading onto 7.5% SDS-PAGE gels.

Immunofluorescence Microscopy—CHO/IR and CHO/IR/IRS-1 cells were incubated with 100 nM insulin for the indicated time intervals. Cells were immediately washed with phosphate-buffered saline containing 1 mM Ca^{2+} and 1 mM Mg^{2+} ($PBS^{Ca,Mg}$) and fixed for 30 min at 22 °C with 4% paraformaldehyde/0.1% glutaraldehyde in $PBS^{Ca,Mg}$. The fixed cells were washed three times with $PBS^{Ca,Mg}$ and permeabilized with PBS containing 0.25% Triton X-100 for 5 min at 22 °C. The permeabilized cells were washed three times with $PBS^{Ca,Mg}$ and incubated overnight at 4 °C with block-solution containing 20 mM Tris-HCl (pH 7.4), 150 mM NaCl, 0.01% Tween 20, 0.02% NaN_3, and 3% BSA. The permeabilized cells were incubated with αIRS-1 antibody (1 μg/ml) or αPY (1 μg/ml) for 3 h at 22 °C and then washed three times 15 min each with 20 mM Tris-HCl (pH 7.4) containing 150 mM NaCl, 0.01% Tween 20, and 0.02% NaN_3 (wash solution). TRITC-conjugated goat anti-rabbit IgG (Sigma) was diluted 1:200 in block solution and incubated with the cells for 2 h at 22 °C. Cells were washed three times with wash solution, 15 min each, and three times with $PBS^{Ca,Mg}$, and rinsed briefly in distilled water before mounting in AFT Systems mounting medium (Behring). Cells were visualized under the fluorescence microscope (Zeiss).

Phosphatidylinositol 3′-Kinase Activity—*In vitro* phosphorylation of phosphatidylinositol was carried out in the immune complexes as described previously (32). Subconfluent CHO cells grown in 100-mm dishes were made quiescent by an overnight incubation in F-12 medium containing 0.5% BSA. The quiescent cells were incubated with insulin (0–100 nM) for 10 min and washed once with ice-cold PBS and twice with 20 mM Tris-HCl (pH 7.5) containing 137 mM NaCl, 1 mM $MgCl_2$, 1 mM $CaCl_2$, and 100 μM Na_3VO_4 (buffer A). The cells were solubilized in 1 ml of buffer A containing 1% Nonidet P-40 (Sigma) and 10% glycerol, and insoluble material was removed by centrifugation at 13,000 × *g* for 10 min. Supernatant was incubated with αIRS-1 overnight at 4 °C, and immune complexes were precipitated from the supernatant with protein A-Sepharose (Pharmacia) and washed successively in PBS containing 1% Nonidet P-40 and 100 μM Na_3VO_4 (three times), 100 mM Tris-HCl (pH 7.5) containing 500 mM LiCl and 100 μM Na_3VO_4 (three times), and 10 mM Tris-HCl (pH 7.5) containing 100 mM NaCl, 1 mM EDTA, and 100 μM Na_3VO_4 (two times). The pellets were resuspended in 50 μl of 10 mM Tris-HCl (pH 7.5) containing 100 mM NaCl and 1 mM EDTA,, and combined with 10 μl of 100 mM $MnCl_2$ and 10 μl of 2 μg/μl phosphatidylinositol (Avanti) sonicated in 10 mM Tris-HCl (pH 7.5) containing 1 mM EGTA. The phosphorylation reaction was started by adding 10 μl of 440 μM ATP containing 30 μCi of [γ-^{32}P]ATP. After 10 min at 22 °C, the reaction was stopped with 20 μl of 8 N HCl and 160 μl of $CHCl_3$:methanol (1:1). The samples were centrifuged, and the lower organic phase was removed and applied to a silica gel thin-layer chromatography plate (Merck) which had been coated with 1% potassium oxalate. Thin-layer chromatography plates were developed in $CHCl_3$:CH_3OH:H_2O:NH_4OH (60:47:11.3:2), dried, and visualized by autoradiography. The radioactivity in spots which co-migrated with PtdIns-4P standard (Sigma) was measured by Cerenkov counting as previously described (32).

Thymidine Incorporation—Freshly seeded CHO Cells were grown for 24 h to 25% confluence in 24-well plates (Nunclon). The cells were washed three times in F-12 medium and incubated 3 days in F-12 medium containing 0.1% BSA. The quiescent cells were incubated at 37 °C for exactly 15 h in F-12 medium containing 0.1% BSA and various concentrations of insulin (Elanco) or 10% fetal bovine serum (Sigma). The cells were then incubated for 1 h in F-12 medium containing 0.1% BSA, 25 mM HEPES (pH 7.4), and 1 μCi/ml of [^{3}H] thymidine (Du Pont-New England Nuclear). The cells were washed three times in ice-cold PBS and solubilized in 2 ml of 0.1% SDS at 22 °C for 1 h, and DNA was precipitated with 2.5 ml of ice-cold 20% trichloroacetic acid, collected on glass filters (Whatman). The precipitate was washed three times with ice-cold 10% trichloroacetic acid and the radioactivity was quantitated by scintillation counting in ACS scintillation mixture (Amersham). All determinations were carried out in triplicate. The data is reported as the relative number of CPM above the basal activity measured in the absence of insulin or fetal bovine serum stimulation.

RESULTS

Expression of IRS-1 mRNA in Rat Tissues—IRS-1 was originally purified and cloned from a rat liver cDNA library (19). To determine whether IRS-1 is expressed in other rat tissues, Northern blot hybridization analysis was conducted using poly(A)$^+$ RNA from various rat tissues. Rat liver mRNA was analyzed with two [^{32}P]cDNA probes derived from the IRS-1 as indicated in Fig. 1. One of the probes encoded 3000 bp from the 5′-end of the IRS-1 cDNA (Fig. 1, *lane a*), and other encoded 1000 bp from the 3′-end (Fig. 1, *lane b*). Both probes detected a doublet band of mRNA from rat liver which migrated near 9.5 kb, suggesting that it was the major mRNA species encoding IRS-1. Two smaller mRNA species of 1.4 and 2.2 kb were variably detected, but these are too small to encode the full-length IRS-1. Poly(A)$^+$ RNA from liver, brain, kidney, muscle, and spleen also revealed a doublet band of about 9.5 kb during screening with the full-length cDNA of IRS-1 (Fig. 1, *lane c–g*). The other lower molecular weight mRNA species were different from tissue to tissue and variably detected, and may represent degradation products or nonspecific hybridization. Thus IRS-1 appears to be translated from two high molecular weight mRNA molecules in a variety of rat tissues.

In Vitro Translation of Rat Liver IRS-1 cDNA—The predicted open reading frame in the cDNA of IRS-1 encodes a 131-kDa protein (19). This predicted size is significantly smaller than expected, as IRS-1 migrates between 165 to 185 kDa during SDS-PAGE (19). Although the cDNA contains several alternate start sites prior to the Kozac initiation sequence (CAGCATGG) which could encode larger species, in-frame termination sites following them make this unlikely. To determine whether the open reading frame accounts for the entire IRS-1 protein, various portions of the IRS-1 cDNA were translated *in vitro* using a rabbit reticulocyte lysate, and the migration of the [^{35}S]methionine-labeled IRS-1 was assessed by SDS-PAGE. In the absence of added mRNA, no detectable [^{35}S]methionine-labeled proteins were detected (Fig. 2*B*, *lane a*). Addition of mRNA transcribed from the full-length IRS-1 cDNA, including the in-frame start and stop codons prior to the Kozac initiation site (species I in Fig. 2*A*), produced a very weakly labeled protein at 92 kDa (Fig. 2*B*, *lane e*). However, deletion of the 5′-end preceding the Kozac initiation site (II and III in Fig. 2*A*) caused the production of several proteins, including a 164-kDa species (Fig. 2*B*, *lanes b–d*). Deletion of 1072 bp from the 3′-end of the mRNA just after the first translation termination site further increased the yield of these proteins (Fig. 2*B*, *lane c*). Anti-IRS-1 antibody (αIRS-1) specifically immunoprecipitated the major [^{35}S]methionine-labeled translation products including the 164-kDa species (Fig. 2*B*, *lanes i–j*), confirming that our cDNA construct encoded IRS-1. The smaller immunoreactive proteins are likely to be partial synthetic products. Nonspecific IgG, antiphosphotyrosine antibody (αPY), and antipeptide antibodies which do not immunoprecipitate IRS-1 did not immunoprecipitate the translation products (Fig. 2*B*, *lanes f, g, k,* and *l*). Thus IRS-1 migration is retarded during SDS-PAGE from a predicted molecular mass of 131 kDa to an apparent molecular mass of 164 kDa, which partially accounts for the discrepancy between the predicted and observed molecular weights.

Expression and Phosphorylation of Rat Liver IRS-1 in Quiescent CHO Cells—The expression of IRS-1 was studied in CHO cells which express 30,000 endogenous rodent insulin receptors or in CHO cells expressing 10^6 human insulin recep-

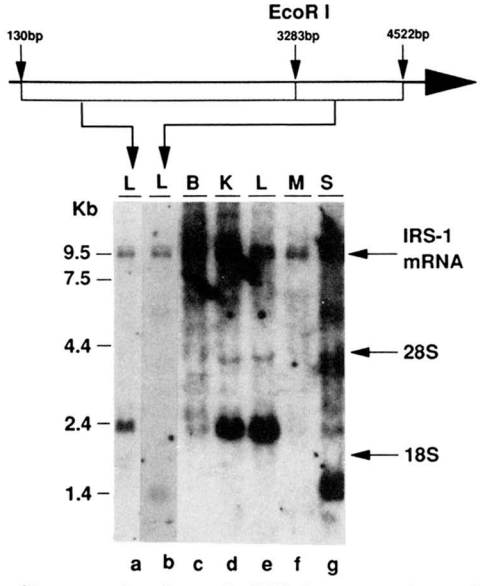

FIG. 1. **Characterization of IRS-1 transcripts.** Rat liver poly(A)$^+$ RNA (10 μg) was denatured, separated by agarose gel electrophoresis, transferred to nitrocellulose membranes, and hybridized separately with two cDNA probes (10^6 cpm/ml) including the 5′-end (*lane a*) or the 3′-end (*lane b*) as indicated in the diagram. (The numbers in the diagram correspond to the IRS-1 cDNA as it was originally described (19)). Poly(A)$^+$ RNA from brain (*lane c*), kidney (*lane d*), liver (*lane e*), muscle (*lane f*), and spleen (*lane g*) were hybridized with full-length IRS-1 c-DNA. The RNA markers are shown on the right. These data are representative of two or three experiments.

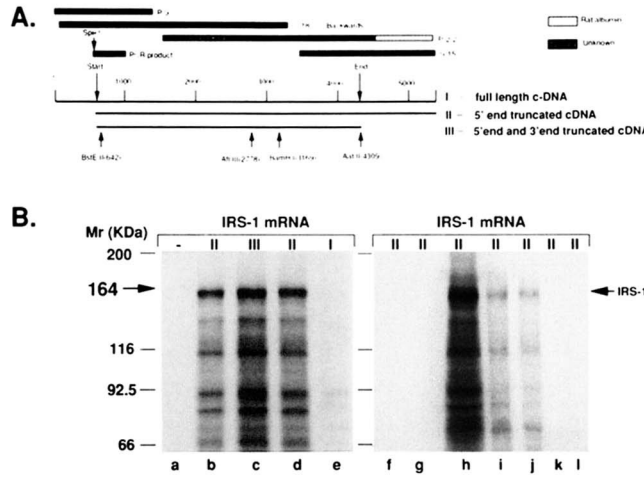

FIG. 2. **Construction of full-length IRS-1 cDNA and *in vitro* translation products of the IRS-1 cDNA.** *A*, *Bst*EII, *Afl*III, and *Aat*II restriction sites in the IRS-1 cDNA were used to construct the full-length IRS-1 cDNA (cDNA I) from cloned fragments. A 5′-end truncated version of this cDNA was prepared by deleting the *Spe*I-*Bst*EII fragment and replacing it with a PCR fragment as described under "Experimental Procedures." Three mRNA molecules were synthesized with this template, all of which contained the putative open reading frame between nucleotide 588 and 4293, but varied in the amount of 5′- and 3′-untranslated region as shown for cDNA molecules I, II, and III. *B*, a reticulocyte lysate was prepared containing no mRNA (*lane a*) or 3 μg of various mRNA molecules (*lanes b–e* and *h*) corresponding to IRS-1 cDNAs shown in *A*. Each reaction was incubated with [^{35}S]methionine for 2 h, and the mixture of proteins was separated by SDS-PAGE and detected by autoradiography. The proteins were immunoprecipitated with various antibodies including rabbit IgG (*lane f*), αPY (*lane g*), αIRS-1 (*lanes i* and *j*), and antipeptide antibodies raised against the sequence EETGSEETMNMDLGPG of IRS-1 (*lane k*) or the sequence LEYYENEK of IRS-1 (*lane l*). *In vitro* transcription and translation data shown are the representative of two experiments.

tors (CHO/IR). Several cell lines expressing nearly equal amounts of IRS-1 either alone (CHO/IRS-1) or with the insulin receptor (CHO/IR/IRS-1) were selected for further analysis. The level of insulin receptor in the CHO/IR/IRS-1 clones was shown by immunoblotting to be equal to the level in CHO/IR cells (~10^6 receptor/cell) (33). Moreover, expression of IRS-1 had no effect on the insulin binding isotherm (data not shown).

Expression of IRS-1 was studied in unstimulated [^{35}S] methionine-labeled CHO cells. Immunoprecipitation of control CHO cells or CHO/IR cells with αIRS-1 revealed many weakly labeled proteins, including some slightly under 200 kDa (Fig. 3*A*, *lanes a* and *c*). When αIRS-1 was used to immunoprecipitate IRS-1 from CHO/IRS-1 cells one new strongly labeled protein was observed which migrated between 165 and 170 kDa during SDS-PAGE (Fig. 3*A*, *lane b*). This protein was attributed to [^{35}S]methionine-labeled IRS-1. A similar increase in the amount of immunoprecipitable IRS-1 was also found in CHO/IR/IRS-1 cells; however, the IRS-1 band from these cells migrated slowly during SDS-PAGE and displayed an apparent molecular mass between 170 to 175 kDa (Fig. 3*A*, *lane d*). The level of IRS-1 expressed in CHO/IRS-1 and CHO/IR/IRS-1 cells was nearly equal, as determined by measuring the radioactivity in each band by scintillation counting (Fig. 3*A*, legend). Thus IRS-1 from unstimulated CHO cells migrated more slowly during SDS-PAGE (165–175 kDa) than unphosphorylated IRS-1 produced in the reticulocyte lysate (164 kDa) (compare Figs. 2 and 3).

The slower migration of IRS-1 immunoprecipitated from quiescent CHO/IR/IRS-1 cells may be due to an increased basal phosphorylation state, as protein phosphorylation frequently retards protein migration during SDS-PAGE. The phosphorylation state of rat liver IRS-1 was studied directly in [^{32}P]orthophosphate-labeled CHO cells, and extracts were immunoprecipitated with either αIRS-1 (Fig. 3*B*) or αPY (Fig. 3*C*). Hamster [^{32}P]IRS-1 was weakly detected in CHO and CHO/IR cells with αIRS-1 (Fig. 3*B*, *lanes e*, *f*, and *i*, *j*). However, rat liver [^{32}P]IRS-1 was strongly detected in αIRS-1 immunoprecipitates from unstimulated CHO/IRS-1 and CHO/IR/IRS-1 cells (Fig. 3*B*, *lanes g* and *k*). Although IRS-1 was expressed at about the same level in both cell lines, IRS-1 in unstimulated CHO/IR/IRS-1 cells showed a 2–6-fold higher basal serine/threonine phosphorylation and a 5-kDa higher molecular mass than in CHO/IRS-1 cells (Fig. 3*B* and Fig. 4, *lanes a* and *c*). These results are consistent with the conclusion that the retarded migration of IRS-1 in unstimulated [^{35}S]methionine-labeled CHO/IR/IRS-1 cells (Fig. 3*A*) reflects the increased basal phosphorylation state.

Insulin-stimulated Phosphorylation of IRS-1 in CHO Cells—Insulin slightly stimulated the phosphorylation of IRS-1 immunoprecipitated from the various [^{32}P]phosphate-labeled CHO cell lines with αIRS-1. The total phosphorylation of IRS-1 increased about 1.2- to 1.3-fold after insulin stimulation (Fig. 3*B* and legend, *lanes e–l*). Phosphoamino acid analysis was carried out on IRS-1 immunoprecipitated from CHO/IRS-1 and CHO/IR/IRS-1 cells. Insulin slightly increased phosphoserine and phosphothreonine in these cells; however, phosphotyrosine was detected only after insulin stimulation, and was strongest in the CHO/IR/IRS-1 cells (Fig. 4, *lanes a–d*). Phosphoserine was the predominant phosphoamino acid before and after insulin stimulation.

Before insulin stimulation, IRS-1 was not immunoprecipitated with αPY from transfected or untransfected [^{32}P]phosphate-labeled CHO cells, confirming that IRS-1 was not tyrosine-phosphorylated before insulin stimulation (Fig. 3*C*, *lanes m*, *o*, *q* and *s*). After insulin stimulation, [^{32}P]IRS-1 was weakly immunoprecipitated with αPY from CHO, CHO/IR, or CHO/IRS-1 cells. The amount of [^{32}P]IRS-1 immunoprecipitated from insulin-stimulated CHO/IR and CHO/IRS-1 cells was 2-fold higher than in control CHO cells, suggesting that the increased amount of kinase or substrate was necessary to detect tyrosine phosphorylated IRS-1 by this method (Fig. 3*C*, *lanes p* and *r*). Expression of both the insulin receptor and IRS-1 in CHO/IR/IRS-1 cells caused a 15-fold increase in the amount of [^{32}P]IRS-1 that was immunoprecipitated with αPY during insulin stimulation relative to the single transfectants (Fig. 3*C*, *lanes r* and *t*). Phosphoamino acid analysis revealed that this remarkable signal was due mainly

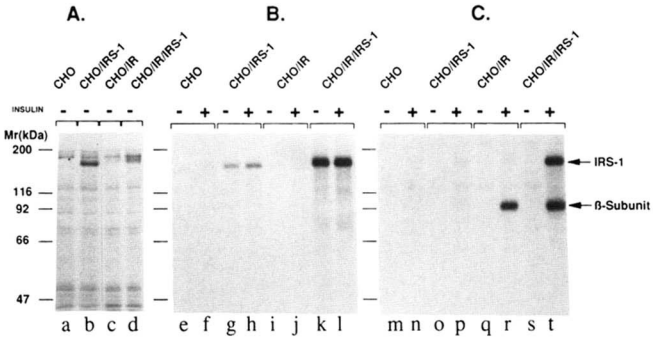

FIG. 3. **Metabolic labeling of CHO, CHO/IR, CHO/IRS-1, and CHO/IR/IRS-1 cells.** Cells were labeled with Trans^{35}S-label overnight or [^{32}P]orthophosphate for 3 h. In some cases the labeled cells were stimulated with 100 nM insulin (+) for 2 min. Cell extracts were prepared and immunoprecipitated with αIRS-1 (*lanes a–l*) or αPY (*lanes m–t*). The immunoprecipitated proteins were reduced with DTT, separated by 7.5% SDS-PAGE, and detected by autoradiography. *A*, αIRS-1 immunoprecipitates of Trans^{35}S-labeled extracts from quiescent cells. Gel fragment which contained IRS-1 band were excised and counted in the scintillation mixture: *lane a*, 397 cpm; *lane b*, 7564 cpm; *lane c*, 420 cpm; *lane d*, 5671 cpm. *B*, αIRS-1 immunoprecipitates of ^{32}P-labeled cell extracts before (−) and after insulin stimulation (+). Gel fragment containing the IRS-1 band were excised, and Cerenkov radiation was measured: *lane e*, 170 cpm; *lane f*, 248 cpm; *lane g*, 932 cpm; *lane h*, 1145 cpm; *lane i*, 271 cpm; *lane j*, 356 cpm; *lane k*, 5529 cpm; *lane l*, 6174 cpm. *C*, an equal portion of extract used in *B* was immunoprecipitated with αPY. Gel fragment containing the IRS-1 band were excised, and Cerenkov radiation was measured: *lane m*, 42 cpm; *lane n*, 149 cpm; *lane o*, 29 cpm; *lane p*, 311 cpm; *lane q*, 33 cpm; *lane r*, 332 cpm; *lane s*, 164 cpm; *lane t*, 5041 cpm. These data are representative of two experiments.

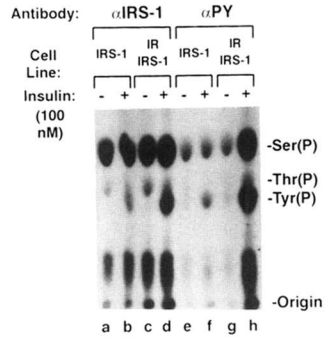

FIG. 4. **Phosphoamino acid analysis of *in vivo* phosphorylated IRS-1 in CHO/IRS-1 and CHO/IR/IRS-1 cells.** [^{32}P]Orthophosphate-labeled CHO/IRS-1 and CHO/IR/IRS-1 cells were incubated with or without 100 nM insulin for 2 min. Phosphorylated IRS-1 was immunoprecipitated from the whole-cell extracts with αIRS-1 or αPY antibody and separated by SDS-PAGE. Phosphoamino acid analysis was performed as described under "Experimental Procedures." The radioactivity (Cerenkov CPM) was measured for each phosphoamino acid (Ser(P)/Thr(P)/Tyr(P)) in *lanes a–h*: *lane a*, 409/11/1; *lane b*, 460/27/16; *lane c*, 771/41/0; *lane d*, 1156/87/236; *lane e*, 53/0/0; *lane f*, 63/2/36; *lane g*, 60/0/4; *lane h*, 1197/117/732. These data are the representative of two experiments.

to the association with the αPY of a highly serine-phosphorylated IRS-1 molecules that contained phosphotyrosine. In contrast, the phosphoserine level of IRS-1 immunoprecipitated with αPY from CHO/IRS-1 was not increased above the background level, suggesting that the endogenous insulin receptors mainly phosphorylated IRS-1 molecules that were not phosphorylated in the basal state (Fig. 4, *lanes e* and *f*).

To determine the complexity of IRS-1 phosphorylation, tryptic peptide mapping was carried out with control and insulin-stimulated CHO/IR/IRS-1 cells (Fig. 5). Before insulin stimulation, 12 phosphoserine-containing HPLC peaks were detected, four also contained phosphothreonine (peaks 2, 6, 10, and 11) and one (peak 20) contained a small amount of phosphotyrosine (Fig. 6*B*). After insulin stimulation, six strong phosphotyrosine-containing peaks were found (peaks 4, 8, 12, 13, 15, and 22), in addition to other weakly tyrosine phosphorylated ones (Fig. 5 and 6*A*). Insulin also stimulated the appearance of several new phosphoserine-containing peaks (peaks 3, 6, 13, 15, 17, 18, 19, and 21), and there was one new peptide containing phosphothreonine (peak 12). Overall, phosphoserine was the major phosphoamino acid found in IRS-1 from CHO/IR/IRS-1 cells before and after insulin stimulation. Thus IRS-1 contains multiple phosphorylation sites and undergoes tyrosine and possibly new serine/threonine phosphorylation at several sites immediately after insulin stimulation.

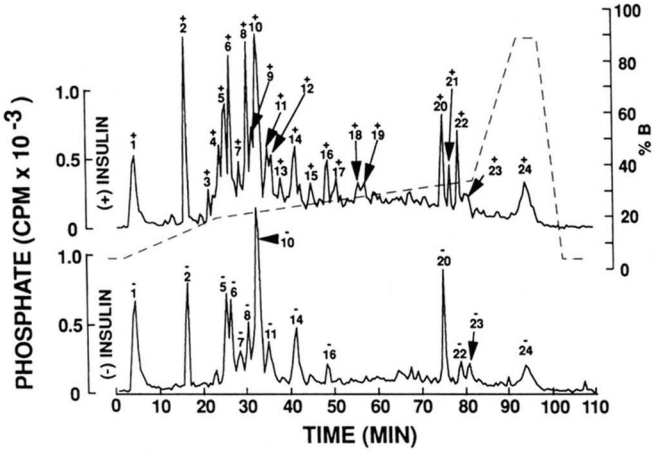

FIG. 5. **HPLC analysis of tryptic phosphopeptides derived from *in vivo* phosphorylated IRS-1.** CHO/IR/IRS-1 cells were labeled with [^{32}P]orthophosphate for 2 h and incubated without or with insulin (100 nM) for 2 min. Cell lysates were incubated with αIRS-1. The phosphorylated IRS-1 was separated by 7.5% SDS-PAGE, and gel fragments containing phosphorylated IRS-1 were excised, digested with trypsin, and separated by reversed-phase HPLC.

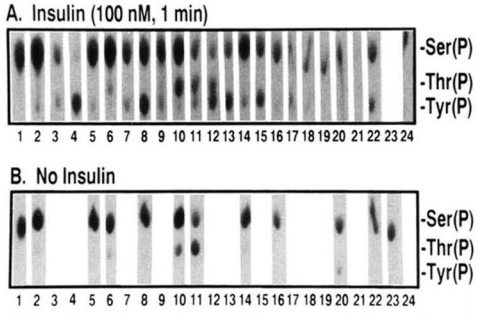

FIG. 6. **The phosphoamino acid composition of each tryptic peptide.** The phosphoamino acid composition of each tryptic peptide shown in Fig. 5 was determined as described under "Experimental Procedures." The numbers under each lane correspond to the peak numbers in Fig. 5.

Time Course of Insulin-stimulated Tyrosine Phosphorylation of IRS-1—The time course of insulin-stimulated tyrosine phosphorylation of IRS-1 immunoprecipitated with αIRS-1 or αPY is difficult to quantify in ^{32}P-labeled cells because of the presence of the predominant serine phosphorylation. In contrast, αPY immunoblotting of cell lysates provides a direct estimate of tyrosine phosphorylation. Before insulin stimulation, CHO cell extracts contained no phosphotyrosine detectable by immunoblotting with αPY (Fig. 7*B*). Immediately after insulin stimulation, the β-subunit of the insulin receptor undergoes tyrosine autophosphorylation, and it is readily detected in CHO/IR and CHO/IR/IRS-1 cells (Fig. 7*B*, *lanes i–p*) and poorly detected in CHO and CHO/IRS-1 cells as they contain few insulin receptors (Fig. 7*B*, *lanes a–h*) (5). Receptor autophosphorylation persisted during 1 h of continuous insulin stimulation, and over expression of IRS-1 did not affect the level of insulin-stimulation β-subunit tyrosine phosphorylation (Fig. 7*B*, *lanes i–p*).

IRS-1 was immunoblotted with αPY from insulin-stimulated CHO/IRS-1, CHO/IR and CHO/IR/IRS-1 cells. The signal was strongest in the CHO/IR/IRS-1 cells (Fig. 7*B*), even though the CHO/IRS-1 and CHO/IR/IRS-1 cells contained nearly equal amounts of IRS-1 (Fig. 7*A*, *lanes e–h* and *m–p*). Before insulin stimulation, rat liver IRS-1 in CHO/IRS-1 and CHO/IR/IRS-1 cells was strongly detected by immunoblotting with αIRS-1, and it migrated between 165 and 170 kDa during SDS-PAGE (Fig. 7*A*). Insulin stimulation decreased the migration of IRS-1 in all cell lines where it could be detected with either αIRS-1 or αPY (Fig. 7). In each case, the apparent molecular mass of IRS-1 increased to 180–185 kDa after 1 h. This molecular mass shift occurred with both endogenous and transfected proteins, but was most pronounced in CHO/IRS-1 and CHO/IR/IRS-1 cells with αIRS-1 blotting. As the entire IRS-1 band shifted to the higher molecular weight, the effect of insulin on the migration of IRS-1 appeared to be complete. The shift in molecular weight of the entire band may indicate that nearly all of the IRS-1 molecules undergo increased phosphorylation during insulin stimulation. The reduced migration was unlikely to be due to tyrosine phosphorylation alone, because it was equally

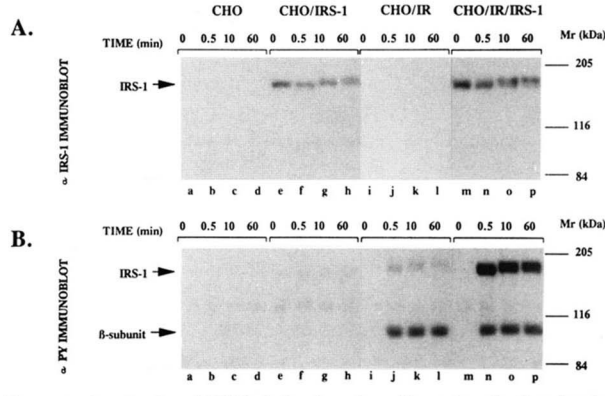

FIG. 7. **Analysis of IRS-1 during insulin stimulation by immunoblotting with αIRS-1 (*A*) and αPY (*B*).** CHO cells were grown to confluence in six-well multi-plates and then stimulated with 100 nM insulin for the indicated time intervals. Stimulation was terminated by discarding the media and adding 300 μl of 1.5 × Laemmli sample buffer containing 150 mM DTT and boiling each sample immediately for 2 min. Lysates were sonicated and 30 μl of each lysate was separated by 6% SDS-PAGE. Proteins were transferred to nitrocellulose paper and probed with the indicated antibody and [^{125}I]protein A. These data are the representative of three experiments.

observed in CHO/IRS-1 and CHO/IR/IRS-1 cells which show significantly different levels of IRS-1 tyrosine phosphorylation (Fig. 7*B*). Moreover, radioactivity in the excised bands indicated that the tyrosine phosphorylation of IRS-1 in the CHO/IR/IRS-1 cells actually decreased 26% after 60 min when the molecular weight showed it greatest increase. It is possible that insulin increases Ser(P) or Thr(P) during prolonged incubations.

The phosphorylation of IRS-1 was also studied *in vitro* using partially purified protein that was produced in Sf9 cells (IRS-1^{bac}) infected with a baculovirus expression vector containing the cDNA of IRS-1. Incubation of IRS-1^{bac} with [γ-^{32}P]ATP and Mn^{2+}, but without the insulin receptor, caused a small amount of serine phosphorylation which was detected by 1 min and increased only slightly during 15 min of continued incubation (Fig. 8, *lanes g–j*). In contrast, incubation of IRS-1^{bac} with the insulin receptor that was previously activated by autophosphorylation strongly increased the phosphorylation of IRS-1^{bac} (Fig. 8, *lanes a–f*). This *in vitro* phosphorylation was slower than the *in vivo* reaction reaching a steady state after 10–15 min (Fig. 8). Phosphoamino acid analysis demonstrated that IRS-1^{bac} was phosphorylated exclusively on tyrosine residues (data not shown), indicating that IRS-1 is a direct substrate of the activated insulin receptor. Interestingly, *in vitro* phosphorylation of IRS-1^{bac} did not cause a dramatic increase in the apparent molecular mass during SDS-PAGE.

Localization of IRS-1 in CHO Cells—IRS-1 is a hydrophilic protein with no stretch of hydrophobic amino acid residues long enough to constitute a transmembrane spanning region. This is consistent with previous work which suggested that pp185 was largely cytosolic (5). To assess the location of IRS-1 in CHO/IR and CHO/IR/IRS-1 cells by fluorescence microscopy, cells were incubated without or with insulin (100 nM) for the indicated time intervals, fixed with paraformaldehyde, and incubated with αIRS-1 or αPY followed by TRITC-conjugated goat anti-rabbit antibody. IRS-1 was not detected above background with αIRS-1 in CHO/IR cells (Fig. 9, *A–D* and *Q*); however, IRS-1 was detected in CHO/IR/IRS-1 cells (Fig. 9, *E–H* and *R*). Before and after insulin stimulation, IRS-1 was absent from the nucleus of CHO/IR/IRS-1 cells, but otherwise uniformly distributed.

Insulin-stimulated tyrosine phosphorylation in the CHO/IR and CHO/IR/IRS-1 cells was also studied by fluorescence microscopy using αPY. Tyrosine-phosphorylated proteins in CHO/IR cells were weakly detected even after 10 min or 1 h of insulin stimulation (Fig. 9, *I–L*). By contrast, there was strong labeling of CHO/IR/IRS-1 cells with αPY after insulin

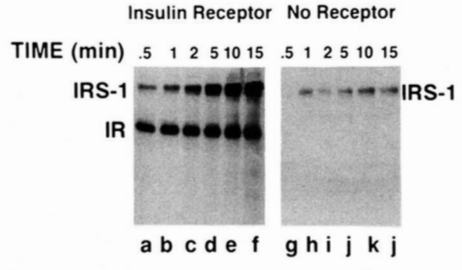

FIG. 8. ***In vitro* phosphorylation of IRS-1^{bac} by wheat germ agglutinin-purified insulin receptor.** Wheat germ agglutinin-purified insulin receptor was autophosphorylated for 20 min by incubation in the presence of 100 nM insulin. IRS-1^{bac} (2 μg) was incubation with 50 μM ATP containing 20 μCi of [γ-^{32}P]ATP in the absence (*lanes g–j*) or presence (*lanes a–f*) of the activated wheat germ agglutinin-purified insulin receptor for the indicated time intervals. Phosphorylated IRS-1 was separated on 7.5% SDS-PAGE gels and detected by autoradiography.

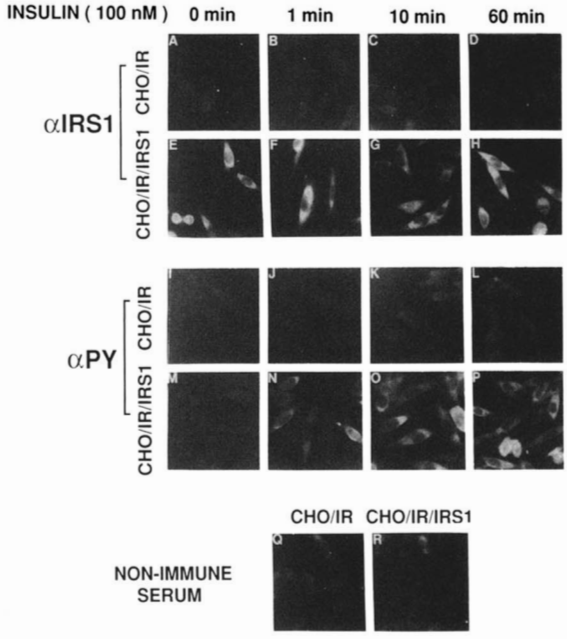

FIG. 9. **Immunofluorescence staining of CHO/IR and CHO/IR/IRS-1 cells with αIRS-1 or αPY antibody.** CHO/IR and CHO/IR/IRS-1 cells were incubated with 100 nM insulin for the indicated time intervals and immediately fixed. The cells were then incubated with nonimmune serum (*Q* and *R*), αIRS-1 (*A–H*), or αPY (*I–P*) for 3 h. After several washes, the cells were incubated with TRITC-conjugated goat anti-rabbit IgG antibody and visualized under the fluorescence microscope.

stimulation; the increased signal probably represents the tyrosine phosphorylation of IRS-1 (Fig. 9, *M–P*). In these cells, the αPY-mediated fluorescent signal appeared most prominent near the plasma membrane after 1 min with insulin (Fig. 9*N*), but became diffusely distributed after prolonged stimulation suggesting that the phosphorylated substrate diffuses throughout the cell.

Association of IRS-1 with the Insulin Receptor in CHO Cells—Although IRS-1 is uniformly distributed throughout CHO cells, some IRS-1 associated with the insulin receptor during insulin stimulation. The association was detected in αIR and αIRS-1 immunoprecipitates from CHO/IR/IRS-1 cell lysates when the immunoprecipitates were washed under mild conditions (50 mM HEPES, pH 7.4, 1% Triton X-100, 150 mM NaCl, 100 mM NaF, 2 mM sodium orthovanadate). After insulin stimulation, αPY immunoblotting indicated that αIRS-1 immunoprecipitates contained both IRS-1 and a small portion (<10%) of the β-subunit of the insulin receptor in these cells; these bands were not found in αIRS-1 immunoprecipitates before insulin stimulation or after insulin stimulation with nonimmune serum (Fig. 10*A*, *lanes a–c*). Furthermore, αIRS-1 immunoprecipitated ^{32}P-labeled IRS-1 and the β-subunit of the insulin receptor (IR-β) from insulin-stimulated cells, whereas only [^{32}P]IRS-1 was immunoprecipitated from unstimulated cells even though the β-subunit is strongly phosphorylated on serine residues before insulin stimulation (Fig. 10*C*, *lanes g* and *h*). Similarly, IRS-1 was specifically detected in αIR immunoprecipitates by immunoblotting with αIRS-1 only after insulin stimulation (Fig. 10*B*, *lanes d–f*). The association between IRS-1 and the activated insulin receptor also occurred *in vitro* during incubation of the baculovirus produced IRS-1 with the activated and autophosphorylated insulin receptor (data not shown). Therefore, during insulin stimulation IRS-1 undergoes tyrosine phosphorylation, and a portion of tyrosine phosphorylated IRS-1 associated with the insulin receptor; however the major portion of

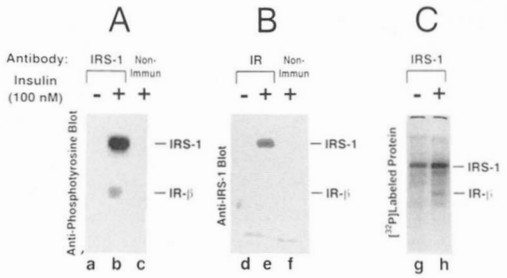

FIG. 10. **Co-immunoprecipitation of the insulin receptor and IRS-1.** CHO/IR/IRS-1 cells were incubated without (−) or with 100 nM insulin (+) for 1 min, and cell lysates were immunoprecipitated with αIRS-1 antibody (*lane a* and *b*), anti-insulin receptor antibody (*lane d* and *e*) or nonimmune serum (*lane c* and *f*). Unlabeled proteins were separated on 7.5% SDS-PAGE gel and transferred to nitrocellulose paper and blotted with αPY (*A*) or αIRS-1 antibody (*B*). [^{32}P]Orthophosphate-labeled proteins (*C*) were immunoprecipitated from control or insulin-stimulated cells with αIRS-1, separated on 7.5% SDS-PAGE, and visualized directly by autoradiography.

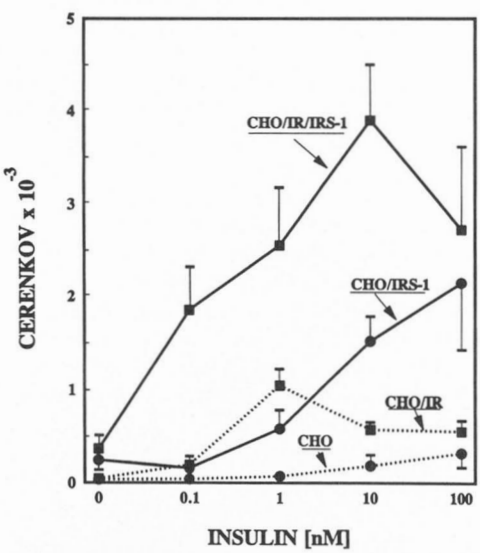

FIG. 11. **Insulin-stimulated association of PtdIns 3′-kinase activity with IRS-1.** CHO, CHO/IRS-1, CHO/IR, and CHO/IR/IRS-1 cells were stimulated with the indicated concentration of insulin for 10 min, and cell extracts were prepared as described under "Experimental Procedures." The PtdIns 3′-kinase activity was assayed in αIRS-1 immune complexes. Values shown are the average of triplicate determinations ± S.D. and represent two experiments.

phosphorylated IRS-1 appears to diffuse throughout the cell based on fluorescence microscopy (Fig. 9).

Effect of IRS-1 on Insulin-stimulated Phosphatidylinositol 3′-Kinase and Thymidine Incorporation—Following insulin stimulation, the phosphatidylinositol 3′-kinase (PtdIns 3′-kinase) associates strongly with IRS-1 and is activated (19, 32, 41). Consistent with this finding, mutant insulin receptors which poorly phosphorylate pp185 (IRS-1) also weakly activate the PtdIns 3′-kinase (24, 32). Moreover, these same mutant receptors weakly mediate insulin-stimulated thymidine incorporation (32). These results with the insulin receptor support previous findings in other systems which suggest that activation of the PtdIns 3′-kinase is related to the regulation of DNA synthesis and cell growth (23).

Insulin strongly stimulated the association of PtdIns 3′-kinase with IRS-1 in CHO/IRS-1 cells. The elevated level of IRS-1 did not affect the half-maximal concentration of insulin (~3 nM), but significantly increased the maximal response (10-fold) compared to the control CHO cells (Fig. 11). In contrast, as shown previously with αPY immunoprecipitates, elevated expression of the insulin receptor alone increased the insulin sensitivity (ED_{50} ~0.3 nM) of the association of activated PtdIns 3′-kinase with endogenous IRS-1, but the maximum response was not significantly increased (Fig. 11). However, in CHO/IR/IRS-1 cells, both effects were observed during insulin stimulation, as the association between IRS-1 and the activated PtdIns 3′-kinase was most sensitive (ED_{50} < 0.1 nM), slightly more responsive than in CHO/IRS-1 cells, and 5-fold more responsive than in CHO/IR cells (Fig. 11).

Insulin stimulated [^{3}H]thymidine incorporation into DNA of control CHO cells with an ED_{50} of about 4 nM. Elevated expression of the insulin receptor alone in CHO/IR cells confirmed previous reports (33, 34) that the sensitivity to insulin increased (ED_{50} = 0.2 nM) (Fig. 12). In contrast, overexpression of IRS-1 alone in the CHO/IRS-1 cells increased by 2-fold the maximum response of thymidine incorporation to insulin stimulation, with no effect on the sensitivity to insulin (Fig. 12). The effect on DNA synthesis of overexpressing the insulin receptor or IRS-1 alone was similar to the effect of insulin on the association of PtdIns 3′-kinase with IRS-1. In contrast, overexpression of the insulin receptor and IRS-1 together inhibited insulin-stimulated thymidine incorporation at the high insulin concentrations (Fig. 12). Although the response to insulin was reduced, the sensitivity to insulin was retained (ED_{50} = 0.2 nM). Thus, elevated levels of IRS-1 has opposite effects on DNA synthesis depending on the concentration of the insulin receptor in the cells. A similar pattern of response was observed during stimulation of cells with 10% fetal bovine serum (Fig. 12, legend). This was opposite to the effect seen with the PtdIns 3′-kinase, where both the response to insulin and the sensitivity to insulin were increased.

Insulin-stimulated thymidine incorporation was also measured in clones expressing different amounts of IRS-1 and nearly equivalent amounts of insulin receptor. CHO/IR/IRS-1 clones 1 and 3, which expressed the highest level of IRS-1 (Fig. 13*A*), showed the strongest inhibition of thymidine

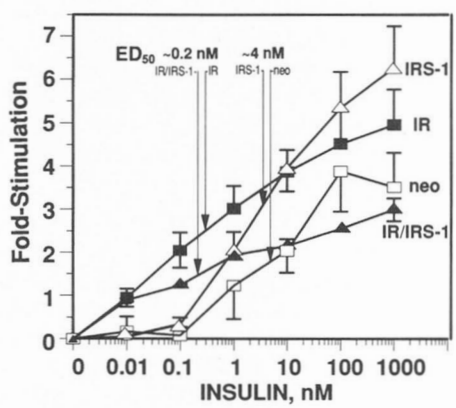

FIG. 12. **Stimulation of thymidine incorporation in CHO cells expressing the insulin receptor and IRS-1.** Subconfluent monolayers of CHO, CHO/IRS-1, CHO/IR, and CHO/IR/IRS1 cells were serum-starved for 72 h in F-12 medium containing 0.1% insulin-free BSA. These cells were then stimulated with the indicated concentrations of insulin in serum-free F-12 medium for 15 h and then labeled with [^{3}H]thymidine for 60 min. Cells were lysed, and DNA was precipitated with trichloroacetic acid, collected by filtration, and counted in a liquid scintillation counter. The averages (± S.D.) of the -fold stimulation above basal for triplicate data pooled from several cell lines is shown: CHO/neo, three experiments using two clones; CHO/IR, four experiments using one clone; CHO/IRS-1, four experiments using two clones; and CHO/IR/IRS-1, eight experiments using four clones. In parallel experiments, 10% fetal bovine serum had the following effects: CHO/neo, 6 ± 1.8; CHO/IR, 8.4 ± 1.0; CHO/IRS-1, 11.5 ± 1.2; CHO/IR/IRS-1, 6 ± 0.6.

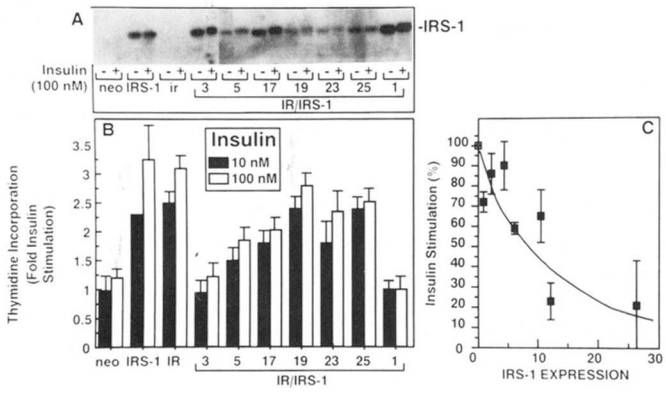

FIG. 13. **Correlation between overexpression of IRS-1 and insulin-simulated thymidine incorporation in CHO cells expressing similar numbers of insulin receptors.** The numbers *1*, *3*, *5*, *17*, *19*, *23*, and *25* correspond to the individual clones that express nearly equivalent amounts of insulin receptor and different amounts of IRS-1. *A*, cells were grown to confluence in six-well multi-plates. After 15 h of starvation, cells were stimulated with or without 100 nM insulin for 1 min and lysed in Laemmli sample buffer. 30 μl of each lysate was separated by 6% SDS-PAGE, transferred to nitrocellulose paper, and immunoblotted with αIRS-1. *B*, cells were stimulated without or with 10 and 100 nM insulin and thymidine incorporation was measured as described in Fig. 12. The data is expressed as the -fold stimulation above basal. Data points are the mean ± S.D. of triplicate determinations, pooled from two experiments. 10% fetal bovine serum had the following effects. CHO/neo: 2.04 ± 0.17; CHO/IRS-1: 5.03 ± 0.47; CHO/IR: 3.55 ± 0.51; CHO/IR/IRS-1: clone-3, 1.38 ± 0.34; clone-5, 2.33 ± 0.19; clone-17, 2.48 ± 0.34; clone-19, 3.54 ± 0.4; clone-23, 2.66 ± 0.44; clone-25, 4.35 ± 0.28; clone-1, 1.17 ± 0.22. **C**, the amounts of IRS-1 in CHO/IR/IRS-1 cell clones from *A* were plotted *versus* insulin-stimulated the thymidine incorporation in each clone. Stimulation of thymidine incorporation in the CHO/IR/IRS-1 clones, expressed as a percentage of the response in CHO/IR cells, was determined at 10 and 100 nM insulin. The data points reflect the mean ± S.D. of the relative stimulation at these two insulin concentrations.

incorporation response to insulin stimulation (Fig. 13*B*), whereas clones 19, 23, and 25, which expressed less IRS-1, have less inhibition in the response to the insulin stimulation. Similar results were obtained after stimulation of these clones with fetal bovine serum (see legend, Fig. 13*B*). The inhibition of thymidine incorporation in response to insulin stimulation showed a striking correlation with the level of IRS-1 in the cells over expressing insulin receptor (Fig. 13*C*).

DISCUSSION

Insulin regulates gene expression, enzyme activity, and cellular growth, but beyond insulin binding and activation of the receptor tyrosine kinase, the elements responsible for signal transmission have been difficult to identify. Naturally occurring mutations which impair the kinase activity of the insulin receptor are associated with severe insulin resistance suggesting that insulin action may be regulated by tyrosine phosphorylation (35, 36). Moreover, various insulin responses such as glucose and amino acid uptake, receptor endocytosis, activation of glycogen synthase, and DNA synthesis are inhibited by mutations that block kinase activity or substrate phosphorylation (4, 34, 37). Direct study of the substrate hypothesis of insulin signaling has been slow because endogenous protein substrates are difficult to observe. During insulin stimulation, the major phosphotyrosine-containing protein found in all cells is the β-subunit of the insulin receptor itself. In addition, a second protein is frequently identified by anti-phosphotyrosine antibody (αPY) which migrates between 165 and 185 kDa during SDS-PAGE. This protein was originally found in Fao hepatoma cells and called pp185 (3). The pp185 was purified from rat liver (18), and its cDNA was isolated from a rat liver cDNA library (19). The cloned protein, called IRS-1, undergoes tyrosine phosphorylation immediately after insulin stimulation and associates with the phosphatidylinositol 3′-kinase (PtdIns 3′-kinase) (19), thereby activating this enzyme (41). Therefore, IRS-1 may be an important intermediate in insulin signal transmission and play a key role in the regulation of cellular growth and metabolism by insulin.

The association between cellular enzymes and growth factor receptor tyrosine kinases is emerging as a common mechanism in signal transduction (23, 38). This phenomena is best characterized for the platelet-derived growth factor and epidermal growth factor receptors which bind certain cellular enzymes following ligand-stimulated autophosphorylation, including phospholipase Cγ, ras-GAP, PtdIns 3′-kinase, and the raf serine/threonine kinase (23). Each of these enzymes contains an isoform of the SH2 (src homology-2) domain, which recognizes and tightly binds to phosphotyrosine residues in a specific amino acid context (22, 39). In the case of the PtdIns 3′-kinase, the SH2 domains in its 85-kDa subunit (p85) bind strongly to phosphotyrosine residues in the kinase-insert region of the platelet-derived growth factor receptor and polyoma middle T antigen (23, 40). These tyrosine residues lie in a similar amino acid sequence motif containing a Y*XX*M motif which forms a high affinity binding site after phosphorylation for the SH2 domains of the PtdIns 3′-kinase. Thus tyrosine kinase receptors act as a "docking" proteins for enzymes which regulate cellular processes (23).

A related mechanism appears to link the insulin receptor to cellular enzymes. IRS-1 associates strongly following insulin stimulation with PtdIns 3′-kinase and this association activates the PtdIns 3′-kinase *in vitro* and *in vivo* (41). These data support the hypothesis that IRS-1 acts as a docking protein to regulates the activity of signal-transducing molecules containing SH2 domain (19). IRS-1 contains at least 14 potential tyrosine phosphorylation sites including 6 located in YM*X*M motifs and 3 in Y*XX*M motifs. Although the exact phosphorylation sites in IRS-1 have not been identified, synthetic peptides based on the sequence around these motifs are excellent substrates for the purified insulin receptor, with K_m values between 20 and 100 μM (21). The fact that IRS-1 undergoes tyrosine phosphorylation at multiple sites based on tryptic peptide mapping, suggests that it may bind to many copies of the PtdIns 3′-kinase causing signal amplification, or it could interact with several distinct SH2 domain containing enzymes to regulate divergent pathways. Moreover, the association between IRS-1 and the insulin receptor may serve to recruit the PtdIns 3′-kinase to the plasma membrane, which may be important for interaction with lipid substrates. Further work is required to identify the exact phosphorylated tyrosine residues that interact with the PtdIns 3′-kinase as well as to identify other enzymes that associate with IRS-1.

We recently utilized mutant insulin receptor molecules to study the role of IRS-1 (pp185) phosphorylation and PtdIns 3′-kinase activation in insulin signal transmission (24, 32). These results suggest that insulin-stimulated PtdIns 3′-kinase activation and stimulation of thymidine incorporation is closely associated with the phosphorylation pp185 (IRS-1) (32). This conclusion is consistent with the results of this study. Over expression of IRS-1 in CHO/IRS-1 cells increases the amount of tyrosine phosphorylated IRS-1 during insulin stimulation. Moreover, the amount of PtdIns 3′-kinase immunoprecipitated from these cells with αIRS-1 is greater. Similarly, insulin stimulation of the PtdIns 3′-kinase is aug-

mented in these cells (41). In parallel, insulin-stimulated thymidine incorporation also increases in the CHO/IRS-1 cells, and the major effect is on the maximum response rather than the sensitivity to insulin. Overexpression of the insulin receptor alone also increases the amount of tyrosine-phosphorylated IRS-1 in CHO/IR cells, but this mainly increases the insulin sensitivity of PtdIns 3′-kinase association with IRS-1 and thymidine incorporation. Overexpression of both IRS-1 and the insulin receptor leads to the expected increase in both sensitivity and response to insulin of PtdIns 3′-kinase activity in αIRS-1 immunoprecipitates. In contrast, the maximum response of thymidine incorporation to insulin in these cells is inhibited, although their sensitivity to insulin is retained. It is unclear why overexpression of both the insulin receptor and IRS-1 has this inhibitory effect. It is possible that the increased serine phosphorylation of IRS-1 found in quiescent CHO cells somehow inhibits signal transmission through IRS-1. As PtdIns 3′-kinase activity in the αIRS-1 immunoprecipitates is not inhibited in the CHO/IR/IRS-1 cells, activation of the PtdIns 3′-kinase by insulin may not be sufficient to increase thymidine incorporation.

IRS-1 may serve during insulin stimulation as a "gathering place" for various signal transduction molecules required for a normal response. When IRS-1 is phosphorylated on YMXM motifs, it associates with certain proteins which contain SH2 domains, such as the PtdIns 3′-kinase. As IRS-1 contains several YMXM motifs, it is possible that other unique signaling molecules associate with IRS-1 to form a signal transduction particle. In addition to the activation of the associated molecules which may occur during binding to the phosphorylated sites, the potential exists in the local environment for interactions between IRS-1-associated molecules. Thus IRS-1 may mediate cross-talk between various molecules that is necessary for the full insulin response. Hyperphosphorylation of an unusually high concentration of IRS-1, which occurs in CHO/IR/IRS-1 cells, may be detrimental for this mechanism, as the density of molecules associated with a single molecule of IRS-1 may be reduced if the concentration of phosphorylated IRS-1 is too high to the point where cross-talk no longer occurs. Moreover, inappropriate molecules may be activated owing to the high concentration of phosphorylated IRS-1 and reduce the response at high insulin concentrations.

IRS-1 is expressed at a low level in many cell and tissues. In the rat, the mRNA encoding IRS-1 is about 9.5 kb. This species is detected with different probes suggesting that it is the major message; however, a slightly higher band is also weakly detected. The cloned cDNA molecule of IRS-1 contains an open reading frame of 3.6 kbp, suggesting that the 9.5-kb mRNA contains a large untranslated region. In contrast, the major mRNA species in a human hepatocarcinoma cell line is 5 kb (20), and a doublet between 6 kb and 6.9 kb in normal human muscle.[3] Rat IRS-1 mRNA is found in liver, kidney, spleen, muscle, and brain, suggesting that IRS-1 is widely distributed. This corresponds to the detection of pp185 previously in these tissues by immunoblotting with αPY after insulin stimulation (18).

The open reading frame of the IRS-1 cDNA has a calculated molecular mass of 131 kDa, which is significantly smaller than the observed size of IRS-1 immunoprecipitated from cells and separated by SDS-PAGE (19). There are three in-frame start codons preceding the Kozac consensus start site (CAGCATGG), which could yield a larger protein; however stop codons in the 5′-untranslated region are expected to block these products. In fact, *in vitro* expression of the cloned cDNA in a rabbit reticulocyte lysate is extremely inefficient when the 5′-untranslated region is included. However, removal of the 5′-untranslated region increased translation nearly 10-fold, and the unphosphorylated [^{35}S]methionine-labeled protein migrates at 164 kDa during SDS-PAGE. In addition, the complete cDNA includes three ATTTA destabilization consensus sequences in the 3′-untranslated region (26), but deletion of this region had no effect on the efficiency of the *in vitro* translation or the size of the unphosphorylated protein products. The molecular mass shift of IRS-1 from a predicted 131 to 164 kDa may be due to certain structural characteristics of IRS-1. Secondary structure predictions using Chou-Fassman algorithms suggest that IRS-1 contains an unusually low α-helix character (4.2% α-helix, 52.1% β-sheet, 22.3% β-turn, and 21.3% random coil) compared with typical globular proteins (30–70% α-helix; 0–30% β-sheet). Thus IRS-1 may fold mainly with β-sheet and random coil structures retarding its migration during SDS-PAGE.

Endogenous IRS-1 is barely detected with αIRS-1 or αPY during immunoblotting or immunoprecipitation from [^{35}S] methionine-labeled CHO cells. In contrast, IRS-1 is readily detected in CHO cells expressing the IRS-1 cDNA (CHO/IRS-1). In quiescent CHO/IRS-1 cells, IRS-1 was strongly serine-phosphorylated, and no phosphotyrosine was detected either by phosphoamino acid analysis or by immunoblotting with αPY. Serine-phosphorylated IRS-1 immunoprecipitated from CHO/IRS-1 cells migrates between 165 and 170 kDa during SDS-PAGE. This represents a small increase compared to IRS-1 synthesized *in vitro*. The difference appears to be due to phosphorylation, as dephosphorylation of IRS-1 immunoprecipitated from CHO cells with alkaline phosphatase reduces its migration to 164 kDa (data not shown). Expression of IRS-1 in CHO/IR cells which contain about 10^6 human insulin receptors causes an unexpected increase (2–6-fold) in the basal serine phosphorylation of IRS-1 and a slightly higher apparent molecular mass. Therefore, overexpression of the insulin receptor may cause, even in quiescent cells, increased expression or activation of a serine kinase which phosphorylates IRS-1. IRS-1 contains over 30 potential sites for serine phosphorylation sites based on consensus sequences for the cAMP-dependent protein kinase, casein kinase II, and protein kinase C (19). Although the exact sites of serine and threonine phosphorylation in IRS-1 are unknown, tryptic peptide mapping suggests that multiple residues are involved. Insulin also stimulates the appearance of several new phosphoserine-containing tryptic peptides. The role of serine phosphorylation in the function of IRS-1 is unknown, but it could provide an important regulatory signal at the IRS-1 locus.

Insulin stimulates tyrosine phosphorylation of IRS-1, which is most readily detected in CHO/IR/IRS-1 cells. A high level of basal serine phosphorylation in IRS-1 obscures the increase in ^{32}P-labeled immunoprecipitates prepared with αIRS-1; however, tryptic peptide mapping and phosphoamino acid analysis clearly shows the presence of phosphotyrosine only after insulin stimulation. Moreover, tyrosine phosphorylation of IRS-1 is readily detected by immunoblotting with αPY, as background serine/threonine phosphorylation does not interfere. In control CHO cells stimulated with insulin, IRS-1 is not detected by immunoblotting with αPY or by immunoprecipitation from ^{32}P-labeled CHO cells with either αIRS-1 or αPY, as previously shown (5, 34). However, it is weakly detected in both CHO/IR cells and CHO/IRS-1 cells, suggesting that the cellular concentration of the kinase or the substrate both affect the level of insulin-stimulated phos-

[3] E. Araki, X. J. Sun, B. L. Haag III, L. M. Chuang, Y. Zhang, T. L. Yang-Feng, M. F. White, and C. R. Kahn, submitted for publication.

phorylation in CHO cells. It is possible that IRS-1 is not directly tyrosine-phosphorylated by the insulin receptor, but instead interacts with an intermediate kinase. However, IRS-1^{bac} purified from Sf9 cells is phosphorylated by the purified insulin receptor exclusively on tyrosine residues, and tryptic peptide mapping indicates that IRS-1 is phosphorylated at multiple sites (data not shown). Further studies will show which tyrosine residues are phosphorylated by the insulin receptor *in vitro* and whether identical tyrosine residues are phosphorylated in the intact cell.

Coincident with insulin-stimulated tyrosine phosphorylation, the molecular mass of IRS-1 increases from 165–170 kDa to 170–175 kDa; after 10 min of insulin stimulation, the apparent molecular mass of IRS-1 increases further and approaches 185 kDa after 1 h. Although the initial increase may be due to tyrosine phosphorylation, the latter changes occur even though the tyrosine phosphorylation of IRS-1 does not increase as detected by immunoblotting with αPY. Furthermore, the molecular weight increase occurs equally in CHO/IR/IRS-1 cells, and in CHO/IRS-1 and CHO/IR cells, even though the latter cell lines do not display strong IRS-1 tyrosine phosphorylation. Denaturation of IRS-1 in 6 M guanidinium HCl has no effect on the migration during SDS-PAGE, whereas dephosphorylation of IRS-1 with alkaline phosphatase reduces the molecular mass to 162–164 kDa (data not shown). Therefore, these changes appear to be due to insulin-stimulated serine/threonine phosphorylation, suggesting that IRS-1 interacts with other insulin-sensitive regulatory molecules which phosphorylate IRS-1 during prolonged stimulation.

Fluorescence microscopy of CHO/IR and CHO/IR/IRS-1 cells suggests that IRS-1 is distributed throughout the cytosol but conspicuously absent from the nucleus. Thus IRS-1 is not a membrane protein as suggested by the absence of a transmembrane spanning region from the primary sequence (19). However, some IRS-1 could be associated with the plasma membrane as a small portion of IRS-1 binds to the insulin receptor following insulin stimulation. At this time, we do not known the molecular basis for this association. IRS-1 is expected to bind to the catalytic domain of the insulin receptor forming an enzyme:substrate complex, but this is expected to be transient and unstable during immunoprecipitation as dissociation of the phosphorylated IRS-1 should be favored. However, the stable association of IRS-1 with the insulin receptor may be important as it brings this molecule and the PtdIns 3′-kinase to the plasma membrane, where it could interact with PtdIns or other molecules involved in signal transmission.

In summary, IRS-1 is expressed in many if not all tissues. Before insulin stimulation, it is phosphorylated on serine and threonine residues. After insulin stimulation, it is tyrosine-phosphorylated on multiple sites and a portion of the IRS-1 associates with the insulin receptor. However, most of the IRS-1 appears to be distributed throughout the cytoplasm of the cell. Tyrosine-phosphorylated IRS-1 binds to the PtdIns 3′-kinase and possibly other enzymes involved in signal transmission. The identification of IRS-1-associated molecules as well as the intrinsic function of IRS-1 and its regulation may provide some of the molecular details of insulin signaling in mammalian cells.

REFERENCES

1. Kahn, C. R., and White, M. F. (1988) *J. Clin. Invest.* **82,** 1151–1156
2. Rosen, O. M. (1987) *Science* **237,** 1452–1458
3. White, M. F., Maron, R., and Kahn, C. R. (1985) *Nature* **318,** 183–186
4. Chou, C. K., Dull, T. J., Russell, D. S., Gherzi, R., Lebwohl, D., Ullrich, A., and Rosen, O. M. (1987) *J. Biol. Chem.* **262,** 1842–1847
5. White, M. F., Stegmann, E. W., Dull, T. J., Ullrich, A., and Kahn, C. R. (1987) *J. Biol. Chem.* **262,** 9769–9777
6. Hofmann, C., White, M. F., and Whittaker, J. (1989) *Endocrinology* **124,** 257–264
7. Margolis, R. N., Schell, M. J., Taylor, S. I., and Hubbard, A. L. (1990) *Biochem. Biophys. Res. Commun.* **166,** 562–566
8. Bernier, M., Laird, D. M., and Lane, M. D. (1987) *Proc. Natl. Acad. Sci. U. S. A.* **84,** 1844–1848
9. Kazlauskas, A., and DiCorleto, P. E. (1987) *J. Cell Physiol.* **130,** 228–244
10. Whittaker, J., Okamoto, A. K., Thys, R., Bell, G. I., Steiner, D. F., and Hofmann, C. A. (1987) *Proc. Natl. Acad. Sci. U. S. A.* **84,** 5237–5241
11. Haring, H. U., White, M. F., Machicao, F., Ermel, B., Schleicher, E., and Obermaier, B. (1987) *Proc. Natl. Acad. Sci. U. S. A.* **84,** 113–117
12. Gibbs, E. M., Allard, W. J., and Lienhard, G. E. (1986) *J. Biol. Chem.* **261,** 16597–16603
13. Maegawa, H., Olefsky, J. M., Thies, S., Boyd, D., Ullrich, A., and McClain, D. A. (1988) *J. Biol. Chem.* **263,** 12629–12637
14. Kadowaki, T., Koyasu, S., Nishida, E., Tobe, K., Izumi, T., Takaku, F., Sakai, H., Yahara, I., and Kasuga, M. (1987) *J. Biol. Chem.* **262,** 7342–7350
15. Shemer, J., Adamo, M., Wilson, G. L., Heffez, D., Zick, Y., and LeRoith, D. (1987) *J. Biol. Chem.* **262,** 15476–15482
16. Momomura, K., Tobe, K., Seyama, Y., Takaku, F., and Kasuga, M. (1988) *Biochem Biophys. Res. Commun.* **155,** 1181–1186
17. Tobe, K., Koshio, O., Tashiro-Hashimoto, Y., Takaku, F., Akanuma, Y., and Kasuga, M. (1990) *Diabetes* **39,** 528–533
18. Rothenberg, P. L., Lane, W. S., Backer, J. M., White, M. F., and Kahn, C. R. (1991) *J. Biol. Chem.* **266,** 8302–8311
19. Sun, X. J., Rothenberg, P., Kahn, C. R., Backer, J. M., Araki, E., Wilden, P. A., Cahill, D. A., Goldstein, B. J., and White, M. F. (1991) *Nature* **352,** 73–77
20. Nishiyama, M., and Wands, J. R. (1992) *Biochem. Biophys. Res. Commun.* **183,** 280–285
21. Shoelson, S. E., Chatterjee, S., Chaudhuri, M., and White, M. F. (1992) *Proc. Natl. Acad. Sci. U. S. A.* **89,** 2027–2031
22. Auger, K. R., Carpenter, C. L., Shoelson, S. E., Piwnica-Worms, H., and Cantley, L. C. (1992) *J. Biol. Chem.* **267,** 5408–5415
23. Cantley, L. C., Auger, K. R., Carpenter, C., Duckworth, B., Kapeller, R., and Soltoff, S. (1991) *Cell* **64,** 281–302
24. Kapeller, R., Chem, K. S., Yoakim, M., Schaffhausen, B. S., Backer, J. M., White, M. F., Cantley, L. C., and Ruderman, N. B. (1991) *Mol. Endocrinol.* **5,** 769–777
25. Sambrook, J., Fritsch, E. F, and Maniatis, T. (1989) in *Molecular Cloning: A Laboratory Manual*, pp. 7.3–7.87, Cold Spring Harbor Laboratory, Cold Spring Harbor, NY
26. Shaw, G., and Kamen, R. (1986) *Cell* **46,** 659–667
27. Innis, M. A., and Gelfand, D. H. (1990) in *PCR Protocols, A Guide to Methods and Applications* (Innis, M. A., Gelfand, D. H., Sninsky, J. J., and White, T. J., eds) pp. 3–12, Academic Press, San Diego
28. Hartman, S. C., and Mulligan, R. C. (1988) *Proc. Natl. Acad. Sci. U. S. A.* **85,** 8047–8051
29. Haring, H.-U., Kasuga, M., White, M. F., Crettaz, M., and Kahn, C. R. (1984) *Biochemistry* **23,** 3298–3306
30. Summers, M. D., and Smith, G. E. (1988) *Tex. Agric. Exp. St. Bull.* **1555,** 1–57
31. Backer, J. M., Schroeder, G. G., Cahill, D. A., Ullrich, A., Siddle, K., and White, M. F. (1991) *Biochemistry* **300,** 6366–6372
32. Backer, J. M., Schroeder, G., Kahn, C. R., Myers, M. G., Jr., Wilden, P. A., Cahill, D. A., and White, M. F. (1992) *J. Biol. Chem.* **267,** 1367–1374
33. Myers, M. G., Backer, J. M., Siddle, K., and White, M. F. (1991) *J. Biol. Chem.* **266,** 10616–10623
34. White, M. F., Livingston, J. N., Backer, J. M., Lauris, V., Dull, T. J., Ullrich, A., and Kahn, C. R. (1988) *Cell* **54,** 641–649
35. Moller, D. A., and Flier, J. S. (1991) *New Engl. J. Med.* **325,** 938–948
36. Taylor, S. I., Kadowaki, T., Kadowaki, H., Accili, D., Cama, A., and McKeon, C. (1992) *Diabetes Care* **13,** 257–279
37. Wilden, P. A., Backer, J. M., Kahn, C. R., Cahill, D. A., Schroeder, G. J., and White, M. F. (1990) *Proc. Natl. Acad. Sci. U. S. A.* **87,** 3358–3362
38. Ullrich, A., and Schlessinger, J. (1990) *Cell* **61,** 203–212
39. Koch, C. A., Anderson, D., Moran, M. F., Ellis, C., and Pawson, T. (1991) *Science* **252,** 668–674
40. Escobedo, J. A., Kaplan, D. R., Kavanaugh, W. M., Turck, C. W., and Williams, L. T. (1991) *Mol. Cell. Biol.* **11,** 1125–1132
41. Backer, J. M., Myers, M. G., Shoelson, S. E., Chin, D. J., Sun, X. J., Miralpeix, M., Hu, P., Marglis, B., Skolnik, E. Y., Schlessinger, J., and White, M. (1992) *EMBO J.* **11,** 3469–3479